



## Future Wireless Communications Empowered by Reconfigurable Intelligent Meta-Materials

**Deliverable 1.1:** Intermediate report on the activities and results of Task  
1.1 – Developing Reconfigurable Intelligent Surfaces.

**Grant Agreement Number:** 956256

**Project Acronym:** METAWIRELESS

**Project Title:** Future Wireless Communications Empowered by Reconfigurable  
Intelligent Meta-Materials

**Funding Scheme:** H2020-MSCA-ITN-2020

**Project Start Date:** 01/12/2020

Type of Document<sup>1</sup>: R

VERSION DETAILS	
<b>Planned Delivery Date:</b>	30 Nov 2022
<b>Original Delivery Date:</b>	30 Nov 2022
<b>Status:</b>	Approved by WP1 leader
<b>Dissemination Level<sup>2</sup>:</b>	PU

PARTICIPANTS	
Participant	Name
AALTO	Sergei Tretyakov, Konstantin Simovski, Javad Shabanpour, Mostafa Movahediqomi
GRW	Jean Baptiste Gros, Vladimir Lenets
DEM-1	Fotis Lazarakis, Fahad Ahmed
WUP-1	Francesco Caminita, Guillermo Encinas Lago
CNIT	Stefano Buzzi, Alessio Zappone

DOCUMENT HISTORY			
Version	Date	Responsible	Description
v1.0	25/11/2022	Stefano Buzzi	First draft
V2.0	30/11/2022	Alessio Zappone	Final Version

DELIVERY REVIEWS			
Version	Date	Reviewed by	Conclusion*

\*e.g., Accepted, Develop, Modify, Re-edit, Update

<sup>1</sup> IN = Information Note; R = Report; P = Prototype; PC = Proof of Concept; O = Other.

<sup>2</sup> PU = Public; CO = Confidential, only for the members of the Consortium (including the Commission Services)

Contents

Executive Summary .....4

List of Project Beneficiaries and Partner Organizations.....5

ACRONYMS.....5

1. Introduction .....5

2. Description of Activities and Results .....8

3. Conclusions .....24

4. Bibliography .....24

## Executive Summary

Deliverable D1.1 of the project Metawireless consists of an intermediate report on the research activities performed within Task 1.1 of WP1.

WP1 is the work package that deals with all the research activities planned by the Metawireless project in order to achieve the technical objectives defined in technical annex of the grant agreement. Specifically, Task 1.1 is concerned with the technical Objective 1, i.e.

*Bring to light the third generation of meta-materials technology by developing reconfigurable intelligent surfaces that can be reconfigured in real-time and are able to perform joint communication and sensing tasks.*

According to the technical annex of the grant agreement, the activities of Task 1.1 comprise an initial phase of literature review to learn the latest theoretical tools and results that have emerged regarding the engineering and modeling of metasurface structures. Afterwards, the research activities will focus on overcoming the state-of-the-art and developing innovative techniques and methodologies for manufacturing and engineering intelligent surfaces that can be reconfigured in real-time.

The rest of this document is organized as follows. Section 1 provides the results of the state-of-the-art review performed during the first phase of Task 1.1. Section 2 describes the ongoing research activities and the innovative contributions achieved by the ERSs, also providing specific references that are key to the research activities performed by each ESR. Finally, concluding remarks are provided in Section 3. All references are provided in Section 4.

## List of Project Beneficiaries and Partner Organizations

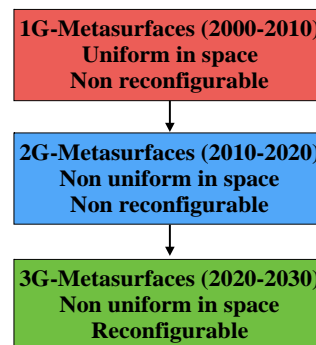
- Aalto-korkeakoulusäätiö (AAL)
- National Centre for Scientific Research "Demokritos" (DEM)
- Greenerwave (GRW)
- Wave Up (WUP)

## ACRONYMS

ESR (s)	Early-Stage researcher(s)
ITN	Innovative Training network
MSCA	Marie Skłodowska-Curie Actions
IPR	Intellectual Property Rights
METAWIRELESS	Future Wireless Communications Empowered by Reconfigurable Intelligent Meta-Materials
WP	Workpackage

### 1. Introduction

Present metasurface structures do not enable a real-time reconfiguration of their electromagnetic response, which limits their use in future wireless networks. The aim of Task 1.1 is to close this gap.



The figure above shows the evolution of metasurface structures. The first generation of metasurfaces could not be reconfigured and was uniform in space. A first improvement came about with the second generation of metasurfaces, which are non-uniform in space, thus allowing to overcome the traditional Snell's laws of reflection. However, also second generation metasurfaces, which represent the current state-of-the-art, are not reconfigurable. The aim of Metawireless is to trigger a new generation of metasurfaces, capable of real-time reconfiguration, and thus allowing to adapt to and compensate the evolution of the wireless channel.

As far as Task 1.1 is concerned, the relevant literature can be grouped into two main areas, i.e. available approaches for metasurface engineering, and studies on their use in mmWave and THz frequency bands, which represent the frequency bands of future wireless networks.

**Metasurface engineering.** Research on metamaterials and metasurfaces has a very long history and countless research contributions can be found in the open technical literature. Background information on *metamaterials* can be found in the books [1], [2], [3], [4]. Notably, a historical perspective on metamaterials can be found in [2]. The theory and applications of *metasurfaces and surface electromagnetics* can be found

in the recent survey papers [5] and [6]. The analytical modeling of applied electromagnetics and scattering theory can be found in [7]. A recent approach to design metasurfaces with multiple reconfigurable functions can be found in [8]. A recent short survey paper on the state-of-the-art of reconfigurable metasurfaces can be found in [9]. A comprehensive survey paper on reconfigurable reflectarrays and array lenses for dynamic antenna beam control is available in [10]. In [11], the authors employ antenna theory to compute the electric field in the near-field and far-field of a finite-size reconfigurable intelligent surface, and prove that it is capable of acting as an anomalous mirror in the near-field of the array. The results are obtained numerically and no explicit analytical formulation of the received power as a function of the distance is given. Similar findings are reported in [12]. In [13], the authors study, through experimental measurements, the power scattered from passive reflectors that operate in the millimeter-wave frequency band. Also, the authors compare the obtained results against ray tracing simulations. By optimizing the area of the surface that is illuminated, it is shown that a finite-size passive reflector can act as an anomalous mirror. In [14], the authors study the path-loss of reconfigurable intelligent surfaces in the far-field regime by leveraging antenna theory. The obtained results are in agreement with those reported in [11] and [12] under the assumption of far-field propagation. In [15], the authors use the scalar theory of diffraction and the Huygens-Fresnel principle in order to model the path-loss in both the near-field and far-field of reconfigurable intelligent surfaces, which are modeled as homogenized sheets of electromagnetic material with negligible thickness. By using the stationary phase method, the authors unveil the regimes under which the path-loss depends on the sum and the product of the distances between the reconfigurable intelligent surface and the transmitter, and the reconfigurable intelligent surface and the receiver. The proposed analytical approach is shown to be sufficiently general for application to uniform reflecting surfaces, anomalous reflectors, and focusing reflecting lenses.

**Metasurface structures for mmWave and THz bands.** In [16], the authors study the application of reconfigurable intelligent surfaces in order to overcome signal path-loss and blind spots in millimeter-wave systems. The problem of maximizing the sum-rate in a multi-user network is addressed by jointly optimizing the transmit beamforming and the reconfigurable intelligent surfaces phase shifts. With the aid of alternating maximization, the resulting two optimization sub-problems are solved in closed-form, and the initial optimization problem is tackled by iterating between them until convergence. The impact of discrete phase shifts is investigated as well, and a projection method is developed to tackle the associated optimization problem. In [17], the authors consider a virtual reality network and study the problem of associating reconfigurable intelligent surfaces to virtual reality users for application in the terahertz frequency band. In particular, the authors formulate a risk-based framework based on the entropic value-at-risk and optimize rate and reliability. The formulated problem accounts for the higher order statistics of the queue length, thus guaranteeing continuous reliability. Tools such as Lyapunov optimization, deep reinforcement learning, and recurrent neural network are adopted to tackle the optimization problem. In [18], the authors propose geometric mean decomposition-based beamforming for application to metasurface-assisted millimeter-wave hybrid MIMO systems. By exploiting the common angular-domain sparsity of millimeter-wave channels over different sub-carriers, an orthogonal matching pursuit algorithm is proposed to obtain the optimal beamforming vector. By leveraging the angle of arrival and angle of departure associated with line-of-sight channels, the authors design the reconfigurable intelligent surface phase shifts by maximizing the array gain for line-of-sight channels. Simulation results show that the proposed scheme achieves better error performance. In [19], the authors consider a metasurface-assisted millimeter-wave communication system in which a reconfigurable intelligent surface is used to overcome the impact of spatial blockages. The objective is to jointly optimize the power of individual devices, the multi-user detection matrix, and the beamforming at the reconfigurable intelligent surface. To this end, new methods for minimizing the power under delay requirements are proposed, and the optimization problem is solved by using alternating optimization. In particular, the configuration of the reconfigurable intelligent surface is formulated as a sum-

of-inverse minimization fractional programming problem, and it is solved by using the alternating direction method of multipliers. The proposed approach is shown to outperform semidefinite relaxation techniques. In [20], the authors consider a metasurface-aided downlink wireless system in the millimeter-wave frequency band and formulate a joint power allocation and beamforming design problem in order to maximize the weighted sum-rate. To solve the problem, the authors propose a novel alternating manifold optimization based beamforming algorithm. Simulation results show that the proposed optimization algorithm outperforms existing algorithms. In [21], the authors consider an indoor communication system for application to terahertz communications and study the application of reconfigurable intelligent surfaces for improving the reliability of signal transmission. The authors study the problem of optimizing the sum-rate performance by selecting the optimal reconfigurable intelligent surface phase shifts. Two algorithms based on a local search method and cross-entropy method are proposed and their performance analyzed with the aid of numerical simulations. In [22], the authors analyze a metasurface-aided millimeter-wave massive MIMO system and show that a proper positioning of the active antennas with respect to the reconfigurable intelligent surface leads to a considerable improvement of the system spectral efficiency. It is revealed that conventional MIMO architectures are either energy inefficient or expensive and bulky if the number of transmit antennas is large. On the other hand, metasurface-aided MIMO architectures are shown to be highly energy efficient and fully scalable in terms of number of transmit antennas. In [23], the authors consider the application of reconfigurable intelligent surfaces in order to alleviate the line-of-sight requirement in free space optical systems. The authors develop conditional and statistical channel models that characterize the impact of the physical parameters of a reconfigurable intelligent surface, which include the size, position, and orientation, on the quality of the end-to-end channel. Furthermore, the authors propose a statistical channel model that accounts for the random movements of the reconfigurable intelligent surface, the transmitter, and the receiver. With the aid of the proposed channel models, the authors analyze the advantages and limitations of reconfigurable intelligent surfaces in different scenarios. In [24], the authors consider the application of reconfigurable intelligent surfaces for improving the channel capacity of millimeter-wave indoor networks. More precisely, the authors propose two optimization schemes that exploit the customizing capabilities of the reconfigurable intelligent surface reflection elements in order to maximize the channel capacity. The first optimization scheme exploits only the adjustability of the reconfigurable intelligent surface reflection elements. For this scheme, approximate expressions of the channel capacity are derived and used to infer the connection between the channel capacity gains and the system parameters. The second optimization scheme jointly optimizes the reconfigurable intelligent surface reflection elements and the transmit phase precoder. For this scheme, the authors propose a low-complexity technique called global co-phasing to determine the phase shift values for use at the reconfigurable intelligent surface. Simulation results show that the optimization of the reconfigurable intelligent surface reflection elements produces significant channel capacity gains, and that this gain increases with the number of reconfigurable intelligent surface elements. In [25], the authors study a millimeter-wave system in which a base station that employs hybrid precoding communicates with multiple single-antenna users through a reconfigurable intelligent surface. The mean square error between the received symbols and the transmitted symbols is minimized by optimizing the hybrid precoder at the base station and the reconfigurable intelligent surface phase shifts. The optimization problem is tackled by resorting to the gradient projection method. The resulting algorithm is shown to be provably convergent to a point that fulfills the first-order optimality conditions of the considered optimization problem. In [26], the authors analyze a single-user downlink millimeter-wave system model in the presence of multiple reconfigurable intelligent surfaces. The transmit beamforming and the reconfigurable intelligent surface phase shifts are optimized by analyzing single-metasurface and multi-metasurface system setups. In the single-metasurface case, the optimal solution that maximizes the signal-to-noise ratio is derived, under the assumption of rank-one channel. In the multi-metasurface case, a sub-optimal solution based on the semidefinite relaxation method is proposed. The authors show that reconfigurable intelligent surfaces provide an effective way for signal focusing that is

potentially useful for applications in the millimeter-wave frequency band. In [27], the authors generalize the study by analyzing the impact of the finite resolution of the reconfigurable intelligent surface phase shifts. In [28], the authors investigate the use of reconfigurable intelligent surfaces for optical communications. In particular, the authors consider a system model in which multiple optical reconfigurable intelligent surfaces are deployed in the environment and are used to build multiple artificial channels in order to improve the system performance and to reduce the outage probability. The authors analyze the impact of three factors that affect the channel coefficients: beam jitter, jitter of the reconfigurable intelligent surfaces, and the probability of obstruction. Based on the proposed model, the authors derive the probability density function of the channel coefficients, the asymptotic average bit error rate, and the outage probability for systems with single and multiple reconfigurable intelligent surfaces. It is revealed that the probability density function contains an impulse function, which causes irreducible error rate and outage probability floors.

## 2. Description of Activities and Results

### 2.1 Contribution of AAL-1 – Overcoming Gap 1.1

The research project of AAL-1 is meant to address the research Gap 1.1 identified in the technical annex of the grant agreement. Specifically, current metasurface structures are not adequate to be integrated in wireless networks due to the fact that the speed at which available metasurfaces can be reconfigured is not fast enough to cope with rapidly varying wireless environments. Also, metasurfaces need to provide different functionalities, e.g. anomalous reflection/refraction, controllable scattering, focusing, and polarization change, in order to grant different services to different classes of users. In order to overcome Gap 1.1, the activity of AAL-1 is focused on developing new tunable metasurface solutions capable of providing innovative functionalities. The considered approach is based on merging the concepts of metasurfaces and meta-gratings. The sparse structure of meta-gratings is meant to simplify the external control of metasurfaces while the versatile functionalities of metasurfaces will enable new functions. Also, planar versions of bianisotropic metasurfaces will be used to eliminate parasitic reflections from reconfigurable focusing and scattering.

The first line of work of AAL-1 has been focused on designing a novel reconfigurable intelligent surface that is angular stable, polarization independent, and that can operate over a broad frequency band. This is anticipated to be key for the successful integration of reconfigurable intelligent surfaces into wireless networks, for the following reasons:

1- Reconfigurable intelligent surfaces should be mounted on different areas where the location of the users changes in real-time. Therefore, the electromagnetic response of each reconfigurable intelligent surface should be stable by changing the incident angle in both uplink and downlink communication. Unfortunately, this important feature is not provided by present metasurfaces. Thus, AAL-1 developed a practical reconfigurable intelligent surface with a stable electromagnetic response with respect to the incident angle. This enables the developed reconfigurable intelligent surface to work with any placement of the access points or the users.

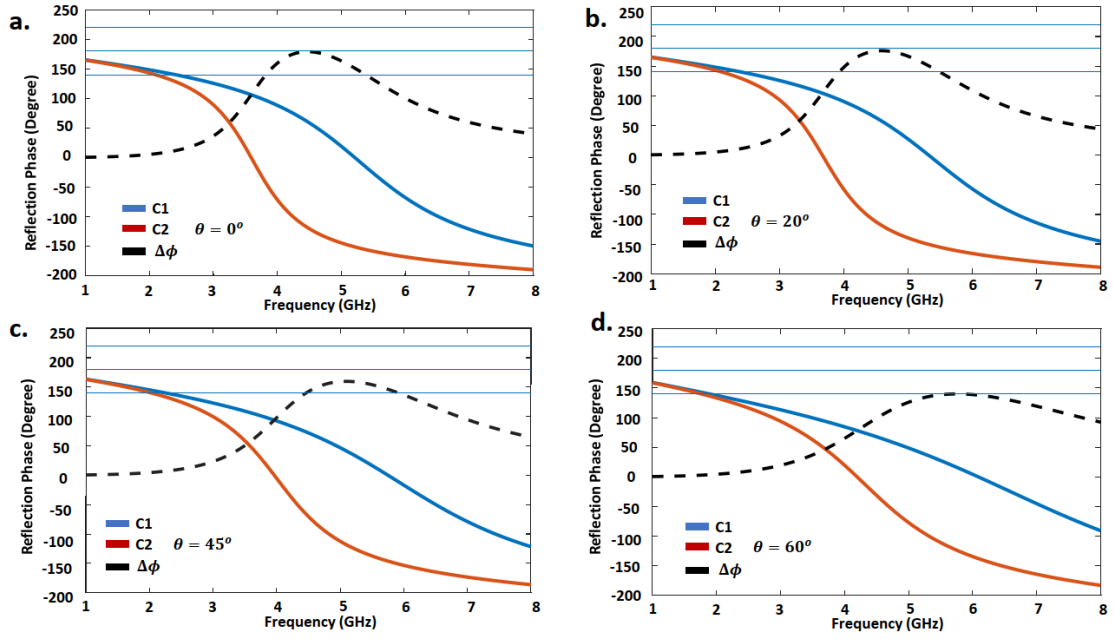
2- In current mobile communication systems, to increase the channel capacity, dual polarization communication is common due to its great advantage. For example, the hybrid polarization communication where both the vertical and horizontal polarization are used together for transferring the information. If a reconfigurable intelligent surface works only for single polarization, then any modulated data on the other orthogonal polarization will vanish after illuminating the surface. So, the polarization stability of reconfigurable intelligent surfaces under different incident angles is a crucial task to form real MIMO mobile



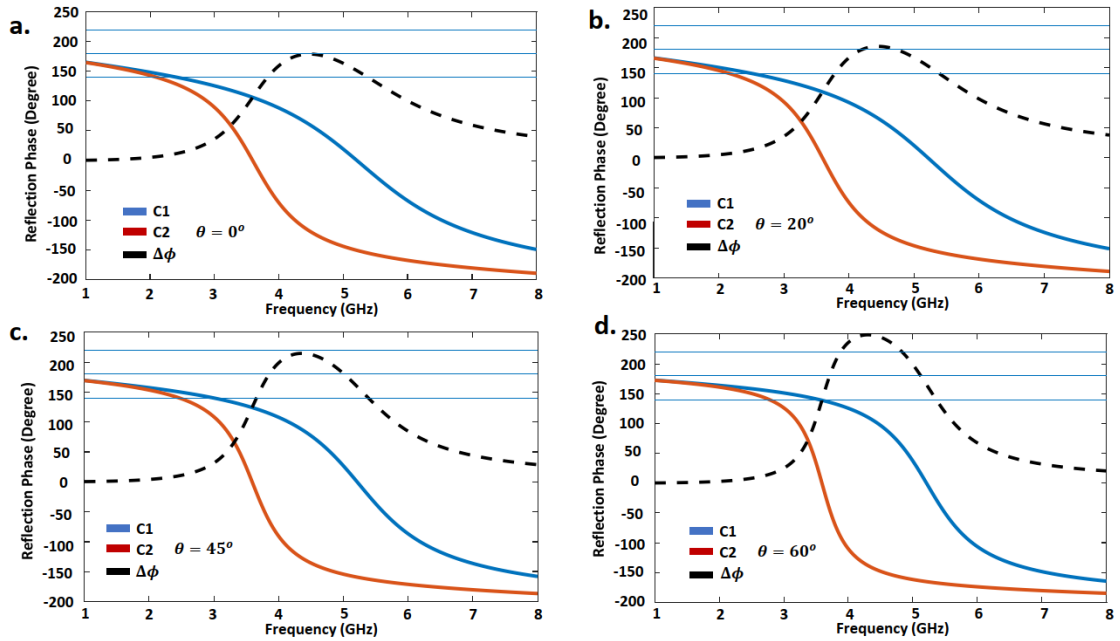
communication systems. The activity of AAL-1 has experimentally verified the polarization stability of the developed reconfigurable intelligent surface under different oblique incident angles.

3- A practical reconfigurable intelligent surface should support transferring data streams through different multiplexing techniques. At least the operation bandwidth of the reconfigurable intelligent surfaces should be larger than each user's signal bandwidth in the Time-division multiplexing (TDM) technique. AAL-1 has developed a broadband reconfigurable intelligent surface which can also keep its electromagnetic response under the non-polarized oblique incident wave.

The stability for Transverse Electric (TE) and Transverse Magnetic (TM) polarizations is shown in the following figures, respectively.

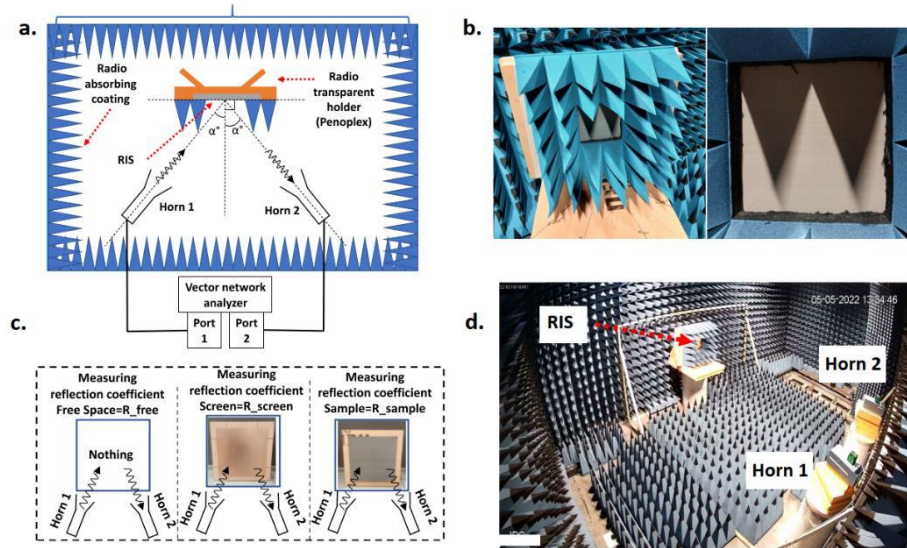


The two-states RPF of our RIS and phase difference  $\Delta\Phi_R$  in the TE case for (a)  $\theta = 0^\circ$ , (b)  $\theta = 20^\circ$ , (c)  $\theta = 45^\circ$  and (d)  $\theta = 60^\circ$ .

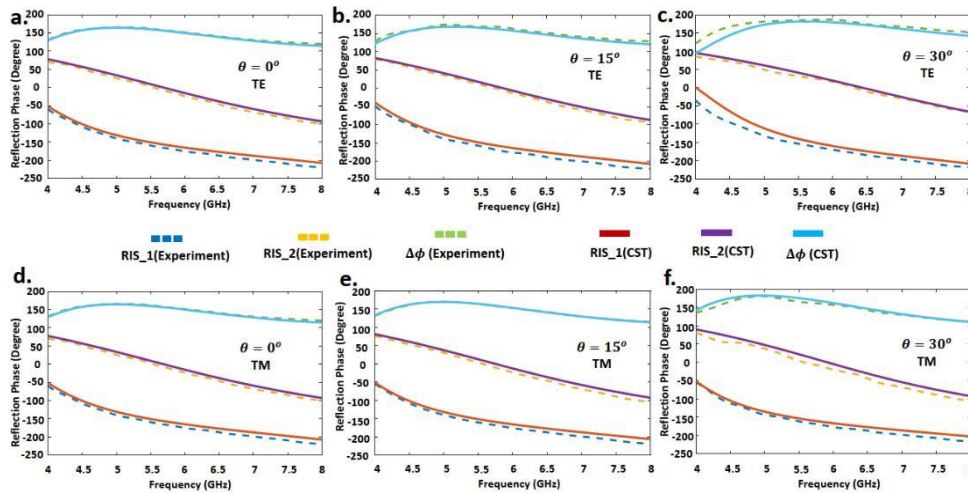


The two-states RPF of our RIS and  $\Delta\Phi_R$  in the TM case for (a)  $\theta = 0^\circ$ , (b)  $\theta = 20^\circ$ , (c)  $\theta = 45^\circ$  and (d)  $\theta = 60^\circ$ .

Next, the following figures show the experimental setup of our design based on the grid of Jerusalem crosses. Fig. (a) shows the measurement setup in the anechoic chamber for evaluating the reconfigurable intelligent surface phase response. Fig. (b) shows the reconfigurable intelligent surface setup that was fabricated. Fig. (c) is a demonstration of three sets of measurements for each incident angle and polarization. Fig. (d) is a 3D view of the experimental setup that was fabricated.



In the picture below, the solid lines and dashed lines represent the results of the CST simulations and experimentation, respectively. As can be observed, the simulated and measured willow-leaf dispersion figures, as well as phase differences, are in good agreement. Eventually, the angular and polarization insensitivity of the developed metasurface design in a broad range of frequencies (32% of bandwidth) is validated through simulation and measurements which proves the effectiveness of the conducted theoretical analysis.



The results of this line of work are currently under review for possible publication in the IEEE Access Journal.

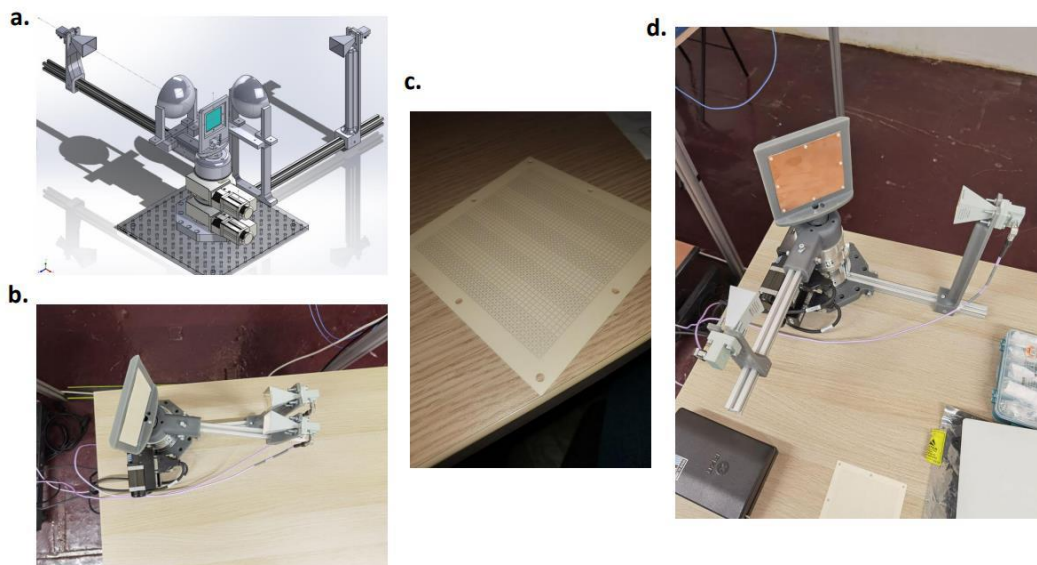
A second line of work of AAL-2 is about showing that using the local reflection coefficient for designing reconfigurable intelligent surfaces based on a phased-array approach will cause serious errors compared to analytical predictions. A reconfigurable intelligent surface that can overcome this limitation has been developed. The relevance of this line of work is further detailed in the following:

1-The authors of [29] studied channel reciprocity using the traditional model and found that channel reciprocity is violated for large deflection angles. In fact, channel reciprocity is an obvious consequence of the general reciprocity theorem. AAL-1 has experimentally verified that the reason for this wrong conclusion lies in the use of the phase-shifter model for a large deflection angle.

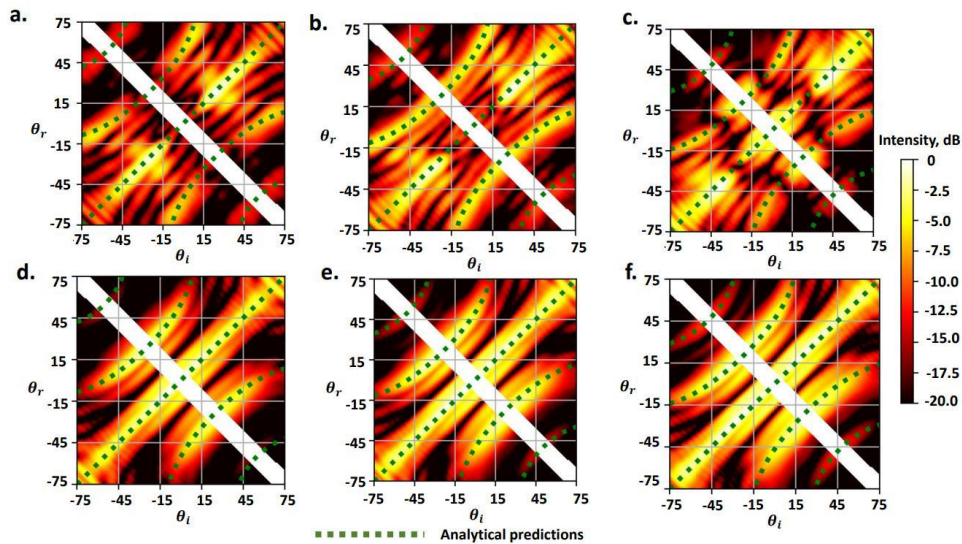
2- To overcome this limitation, AAL-1 has designed a practical binary reconfigurable intelligent surface for reflecting the incident wave. This new design has been experimentally shown to closely follow the approximation of physical optics up to very large incidence angles ( $70^\circ < \theta_i < 70^\circ$ ) for both polarizations.

3- These results enable to create a line of sight between users and access points through the metasurface in a much wider range of angular directions.

In the following, experimental results for this line of work are shown. Specifically, Fig (a) shows a 3D view of the measurement setup. Fig (b) shows the remote-controlled rotating platform with the proposed reconfigurable intelligent surface design, and (d) with the ground plane. Fig (c) shows the fabricated binary reconfigurable intelligent surface with four periods.



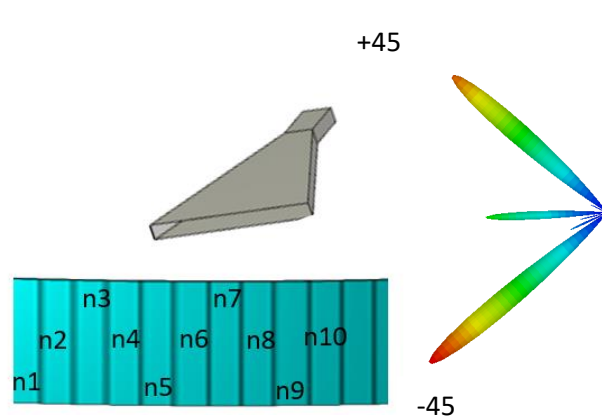
From the figure below, it can be seen that the scattering patterns follow the simplistic analytical predictions very well (in the TM case almost ideally). It is worth noting that by dividing the results into two areas (with respect to the specular direction line), the symmetries of the scattered power are visible. This shows the channel reciprocity of the developed metasurface. Additional experimental results also agree with numerical simulations, thus further validating the applicability of the developed theoretical model of the metasurface. Specifically, the figure shows the refracted intensity color maps for TE polarized incident waves at: (a) 16GHz, (b) 17GHz, (c) 18 GHz, and for the TM polarized incident wave at the same frequencies (Fig. (d)-(f)).



## 2.2 Contribution of DEM-1 – Overcoming Gap 1.2

The research project of DEM-1 is meant to address the research Gap 1.2 identified in the technical annex of the grant agreement. Specifically, present designs of metasurface structures are restricted to narrowband bandwidth operation. This is a barrier to be overcome in order to leverage the gains promised by higher frequencies. In order to overcome Gap 1.2 the approach described below has been used.

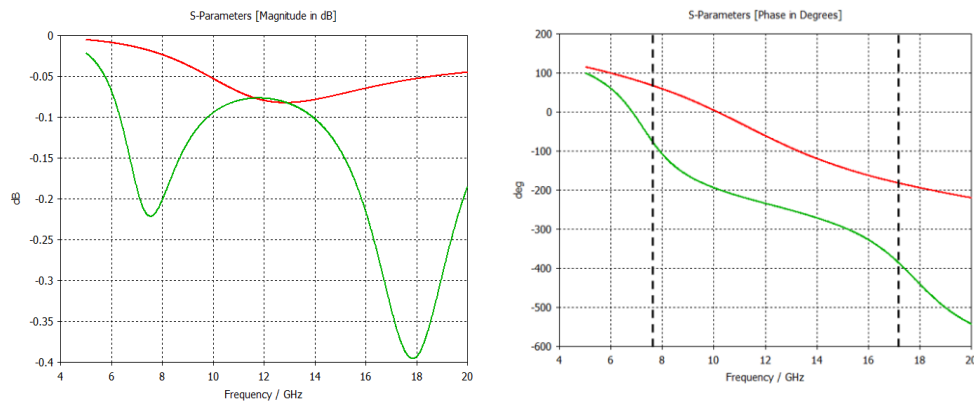
To begin with, the refractive index values for steering beam or achieving beam splitting can be retrieved through MATLAB code by defining the frequency range, steer angle, size of the unit cell, height of the unit cell. DEM-1 proceeded with the design of a simple array of user-defined material and assigned refractive index values to achieve the desired functionality at CST MW studio 2021. Here at this stage, DEM-1 de-embedded the Floquet port on the unit cell and retrieved the phase values from refractive indexes. At ON state and OFF state, a total of  $180^\circ$  phase difference is achieved. The  $0^\circ$ -phase achieved against a 5.35 refractive index, and the  $180^\circ$  phase against a 10.5 value of refractive index.



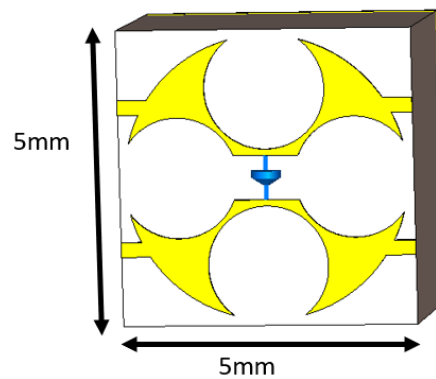
Simulation in CST with user defined material using different refractive index



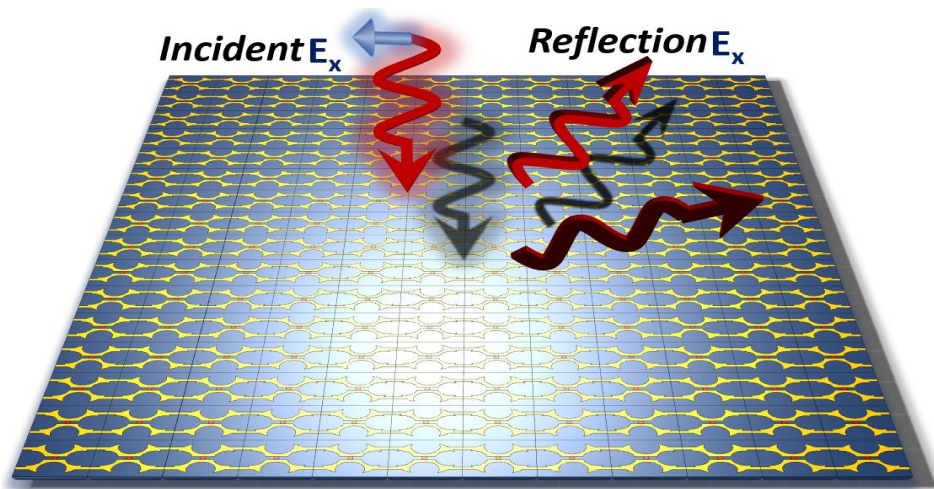
The unit cell is designed in CST MW studio 2021. The PIN diode is used to control the ON and OFF state. At ON and OFF states, the proposed unit cell achieves the same refractive index values, thus giving two phase states with a phase difference of  $180^\circ \pm 20^\circ$ .



Magnitude and Phase difference of ON and OFF states



The Proposed Unit Cell



The Phase gradient Metasurface

The phase gradient metasurface is designed to achieve the beam steering and beam splitting functionalities using different coding sequences. The coding metasurface is comprised of  $N \times N$  super meta-atoms cells, and if the electromagnetic wave is normally incident on it, then the equation of far-field radiation pattern can be written as

$$F(\Theta, \Phi) = \sum_{m=1}^N \sum_{n=1}^N A e^{i \left[ \left( \frac{2\pi}{\lambda} L \left( m - \frac{1}{2} \right) \sin \Theta \cos \Phi + \frac{2\pi}{\lambda} L \left( n - \frac{1}{2} \right) \sin \Theta \sin \Phi \right) + \Phi(m, n) \right]} \quad (1)$$

The  $|F(\Theta, \Phi)|$  function (far field radiation pattern) will attain the maximum value if and only if  $(\Phi)$  azimuth angle and  $(\Theta)$  elevation angle fulfil the following conditions

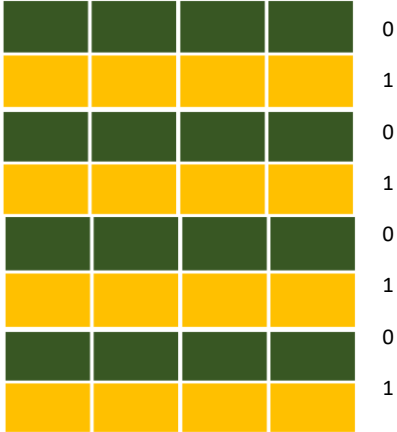
$$\Phi = \pm \arctan \frac{\Gamma_x}{\Gamma_y}, \Phi = \pi \pm \arctan \frac{\Gamma_x}{\Gamma_y} \quad (2)$$

$$\Theta = \arcsin \left( \lambda \sqrt{\frac{1}{\Gamma_x^2} + \frac{1}{\Gamma_y^2}} \right) \quad (3)$$

The physical dimension (periodic length) of the coding sequence (phase gradient) along the y and x directions are  $\Gamma_y$  and  $\Gamma_x$  respectively.

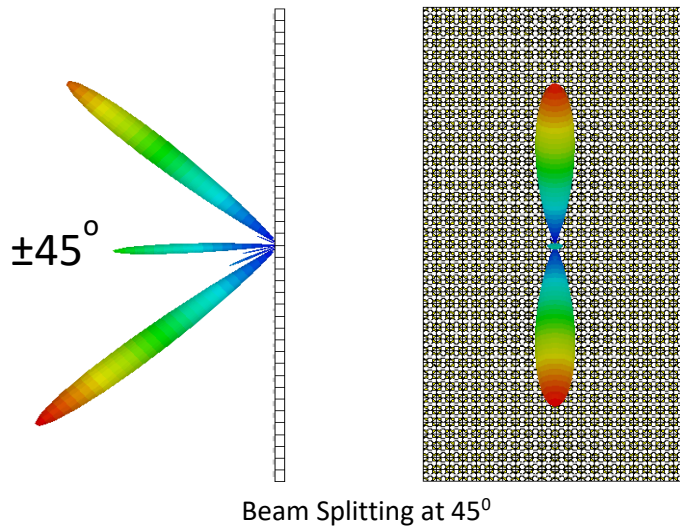
Firstly, two matrices  $\Phi_{ON}$  and  $\Phi_{OFF}$  are defined for representing supercells, then the coding sequence for the simplest case is considered. The coding sequence of supercells (i.e.,  $\Phi_{ON}$  and  $\Phi_{OFF}$ ) and the complete phase gradient metasurface array, which is represented by  $\psi_1$ , are shown in the figure below.

$$\Phi_{ON} = \begin{bmatrix} 0 & 0 & 0 & 0 & 0 \\ 0 & 0 & 0 & 0 & 0 \\ 0 & 0 & 0 & 0 & 0 \\ 0 & 0 & 0 & 0 & 0 \end{bmatrix} \quad \Phi_{OFF} = \begin{bmatrix} \pi & \pi & \pi & \pi & \pi \\ \pi & \pi & \pi & \pi & \pi \\ \pi & \pi & \pi & \pi & \pi \\ \pi & \pi & \pi & \pi & \pi \end{bmatrix}$$

$$\psi_1 = \begin{bmatrix} [\Phi_{ON}] & [\Phi_{ON}] & [\Phi_{ON}] & [\Phi_{ON}] \\ [\Phi_{OFF}] & [\Phi_{OFF}] & [\Phi_{OFF}] & [\Phi_{OFF}] \\ [\Phi_{ON}] & [\Phi_{ON}] & [\Phi_{ON}] & [\Phi_{ON}] \\ [\Phi_{OFF}] & [\Phi_{OFF}] & [\Phi_{OFF}] & [\Phi_{OFF}] \\ [\Phi_{ON}] & [\Phi_{ON}] & [\Phi_{ON}] & [\Phi_{ON}] \\ [\Phi_{OFF}] & [\Phi_{OFF}] & [\Phi_{OFF}] & [\Phi_{OFF}] \\ [\Phi_{ON}] & [\Phi_{ON}] & [\Phi_{ON}] & [\Phi_{ON}] \\ [\Phi_{OFF}] & [\Phi_{OFF}] & [\Phi_{OFF}] & [\Phi_{OFF}] \end{bmatrix}$$


Development of coding Sequence

The coding sequence of 01010101 in the phase gradient metasurface split the beam into  $\pm 45^\circ$  as shown in figure below.



Beam Splitting at  $45^\circ$

In order to attain beam splitting other than  $\pm 45^\circ$ , different coding sequences are applied. To enhance the range of beam scanning through coding metasurface, the supercell of  $5 \times 5$  is replaced by  $5 \times 3$  and coding sequence of 010101010101 is applied. It is interesting to mention here that at 9 GHz the two beams are generated at  $\sim \pm 73^\circ$ .

The maximum perfect beam splitting is achieved up to  $75^\circ$ .

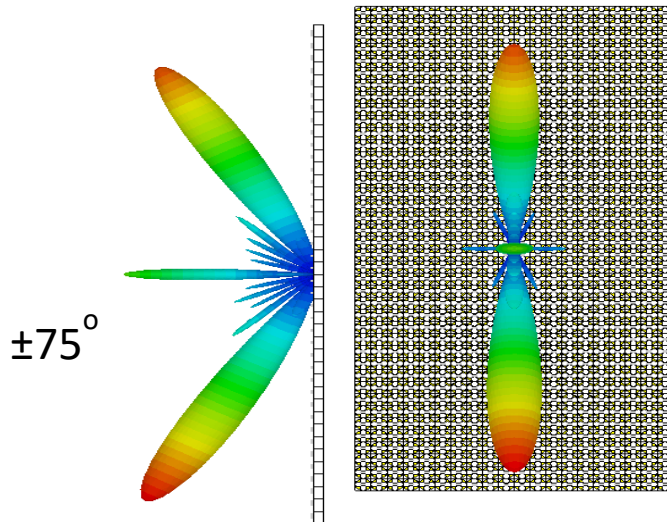


Fig. 7. Beam Splitting at  $75^\circ$

Similarly, the beam is tilted at  $86^\circ$ , when 1001010001 coding sequence is applied in phase gradient surface, but 40% of the wave is reflected at the incidence angle.



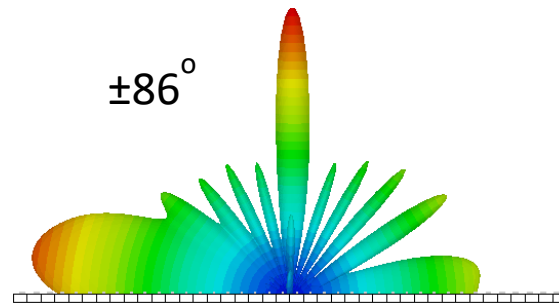


Fig. 9. Beam Splitting at  $86^\circ$

Moreover, multiple beams (4-beams) are generated in the scanning range of  $3^\circ$ - $7^\circ$  and  $6^\circ$ - $12^\circ$  at 9 GHz and 11.6 GHz frequency band respectively when 00111100 sequence is applied as depicted in the figure below.

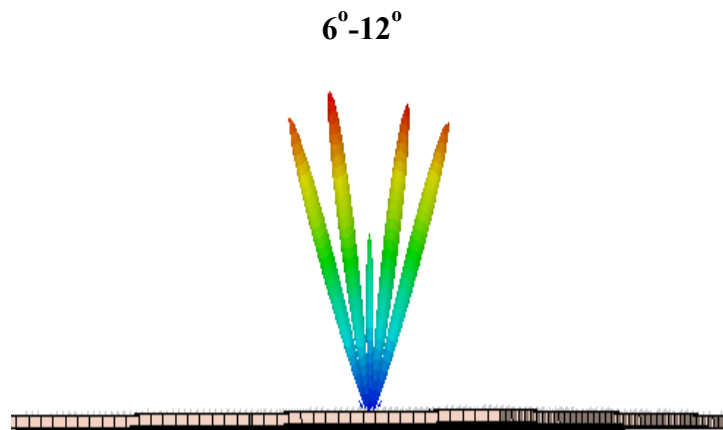


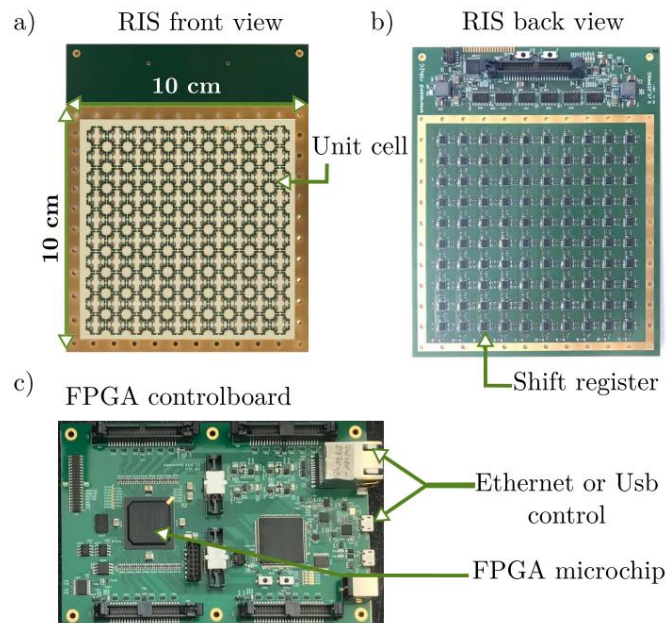
Fig. 8. Four beams are generated with 00111100 sequence at 11.6 GHz

A substrate has been selected, and 1-bit metasurface is under the fabrication process. Once the metasurface is fabricated, measurements will be performed in the anechoic chamber available at DEM to verify the simulation results.

### 2.3 Contribution of GRW-1 – Overcoming Gap 1.3

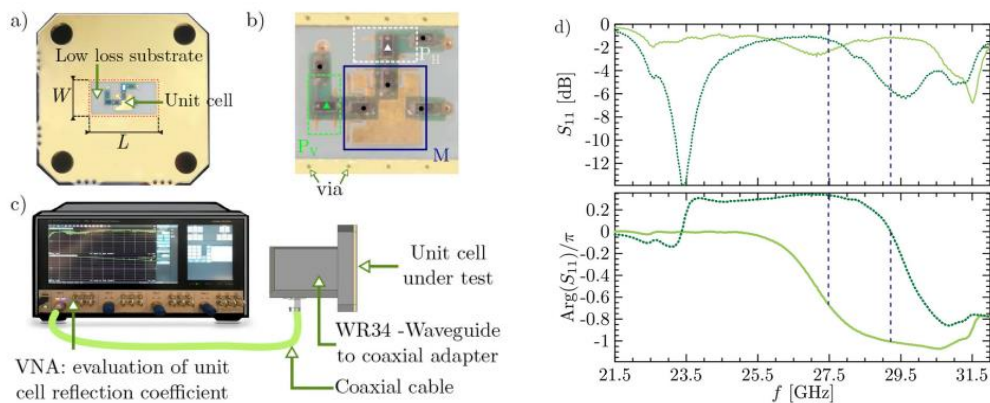
The research activities of GRW-1 are meant to address the research Gap 1.3 identified in the technical annex of the grant agreement. Specifically, present metasurface technologies require a power supply and a microcontroller or FPGA-based control unit to power the reflecting elements. However, this approach is difficult to scale, limiting the size of meta-surfaces, which in turn limits the gains in terms of both communication and sensing performance. In order to overcome Gap 1.3, the research activity of GRW-1 is focused on the development of novel control methods for meta-surfaces that should be deployed with minimum infrastructure cost, and capable of operating also at higher frequencies than sub-6GHz bands. For high-frequency applications, very low complexity and very low power consumption meta-surfaces will be designed and manufactured. Current methods based on GaAs or AlGaAs are, in fact, not appropriate because of their high cost and power consumption.

GRW-1 has developed various reconfigurable intelligent surfaces for different applications. A first line of work has led to the design and demonstration of a reconfigurable intelligent surface for Ka-Rx and Ka-Tx frequency bands. The developed reconfigurable intelligent surface architecture is shown in the figure below.

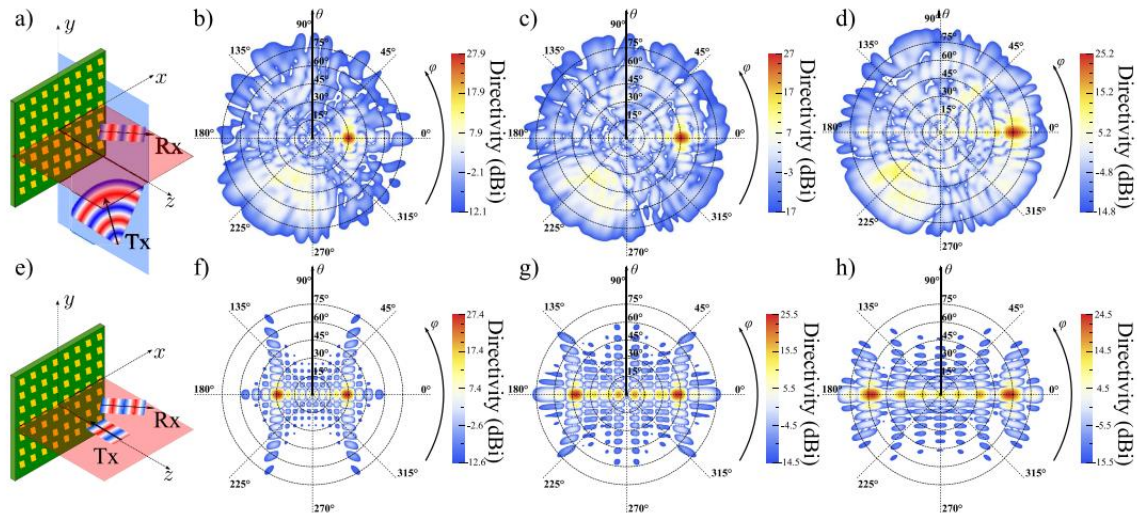


a) Front and b) back side of the fabricated  $10 \times 10 \text{ cm}^2$  reconfigurable intelligent surface. c) reconfigurable intelligent surface control board with different interfaces.

The electromagnetic properties of the reconfigurable intelligent surface have been studied, from its unit cells to full-size device applications in far to far-field configuration and near- to far-field configuration or reflectarray configuration (see the first three figures below).



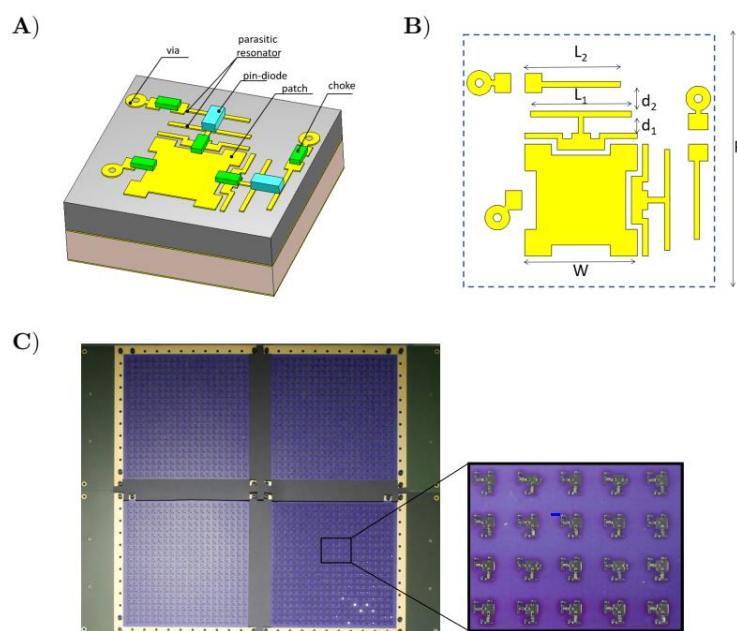
a) Pixel fabricated for the waveguide characterization. The large copper area is intended to form electrical contact with the waveguide flange. b) Magnified photo of the fabricated pixel. The vias around provide isolation of the field inside waveguide. M, PH and PV are main patch, horizontal and vertical parasitic resonator respectively. Dots and triangles tag respectively chokes and pin diodes. c) The setup of the experiment. d) Measured reflection from the single pixel inside the rectangular WR-34 waveguide. Solid line represents OFF-state and dotted line represents ON-state of the pixel. Vertical dashed lines correspond to frequency where actual  $\pi$ -phase shift occurred showing the operating frequency range of the pixel.



(a) Illustration of a spherical wave impinging the reconfigurable intelligent surface and a plane wave being reflected. (b)–(d) Results of the analytical model for the far-field radiation pattern created by the reconfigurable intelligent surface for different configurations defined by steering directions:  $\theta_{Rx} = 30^\circ, 45^\circ$  and  $60^\circ$  are shown ( $\phi_{Rx}$  is  $0^\circ$ ). The Tx antenna is at  $DTx = 145$  mm,  $\theta_{Tx} = 45^\circ$  and  $\phi_{Tx} = 270^\circ$ . (e) Illustration of a plane wave impinging the reconfigurable intelligent surface and a plane wave being reflected. (f)–(h) Results of the analytical model for far-field radiation patterns created by the reconfigurable intelligent surface for different configurations defined by steering directions:  $\theta_{Rx} = 30^\circ, 45^\circ$  and  $60^\circ$  are shown ( $\phi_{Rx}$  is  $0^\circ$ ).

The results of this first line of work have been published in the following paper:

J.-B. Gros, V. Popov, M. A. Odit, V. Lenets and G. Lerosey, *A Reconfigurable Intelligent Surface at mmWave Based on a Binary Phase Tunable Metasurface*, in IEEE Open Journal of the Communications Society, vol. 2, pp. 1055-1064, 2021,



The perspective view (A) and layout (B) of the reconfigurable intelligent surface unit cell. (C) Photo of the fabricated 20cm × 20cm reconfigurable intelligent surface composed of 4 10cm × 10cm reflect arrays, controlled by one FPGA board. The total number of unit cells is 1600, each with independent control of 2 polarisations.

After working on the electromagnetic properties of the developed reconfigurable intelligent surface, a second line of investigation has addressed its performance when placed in a wireless communication link. Specifically, an indoor telecommunication experiment was performed, as shown in the figure below. The experiment emulated a non-line-of-sight scenario consisting of a receive antenna and a transmit antenna, which communication through the reconfigurable intelligent surface structure developed before and by employing a software-defined radio (SDR).

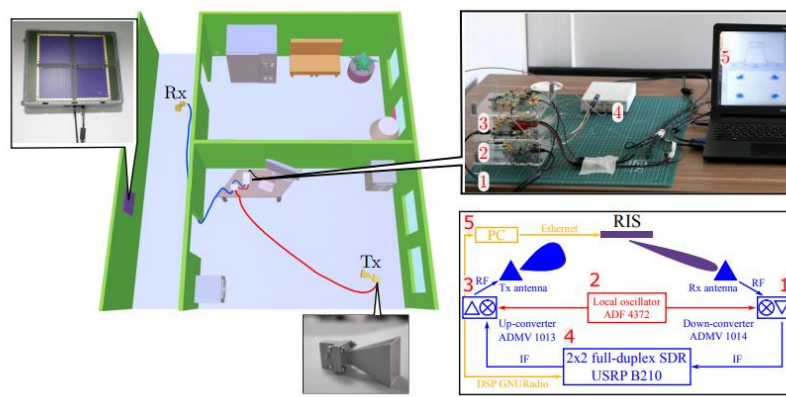


Figure 5. Left: A 3D illustration of the experimental setup used to demonstrate metasurface-aided indoor wireless communication in an NLOS situation. Right: A photograph (top panel) and a schematic (bottom panel) of the communication module represented by a down-converter 1, a local oscillator 2, an up-converter 3, an SDR 4, and a PC 5.

The results of the experiment are shown in the figure below.

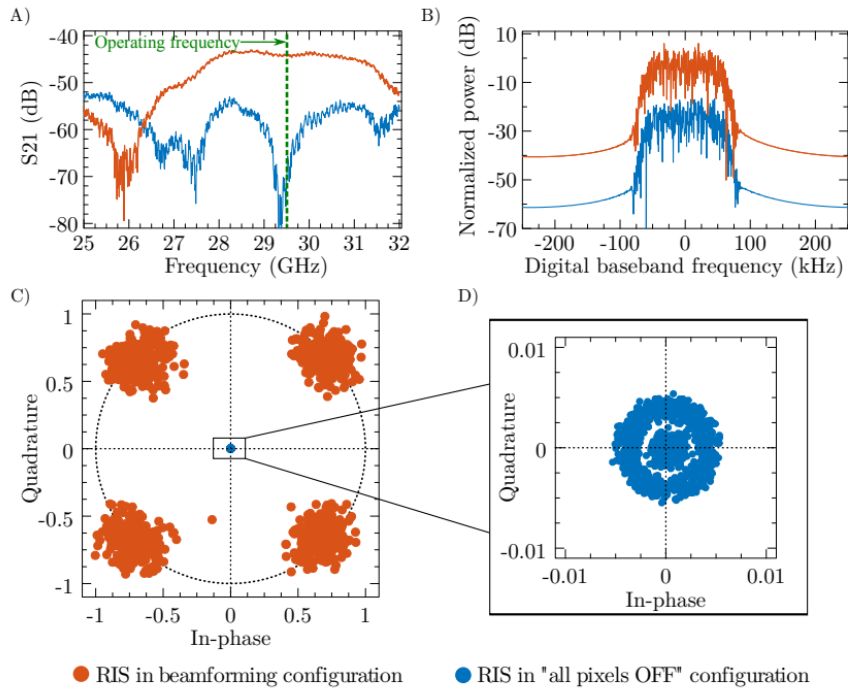
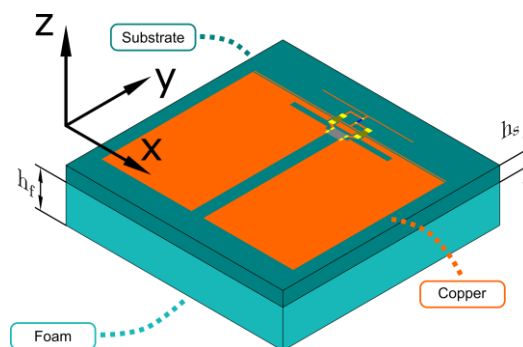


Figure 6. (A) S21 parameter measured with a VNA for channel characterization in two configurations of the reconfigurable intelligent surface: all pixels off and beamforming configuration. (B) The signal received by the SDR and put through an RRC filter, when the reconfigurable intelligent surface is off and on. (C) Constellation diagram after timing recovery, equalization and phase and frequency offset compensation, when the reconfigurable intelligent surface is off and on. (D) Close-up of the constellation diagram when the reconfigurable intelligent surface is off.

The results of this work have appeared in the following paper:

V. Popov, M. Odit, J.-B. Gros, V. Lenets, A. Kumagai, M. Fink, K. Enomoto, and G. Lerosey G, *Experimental Demonstration of a mmWave Passive Access Point Extender Based on a Binary Reconfigurable Intelligent Surface*, Front. Comms. Net 2:733891, 2021.

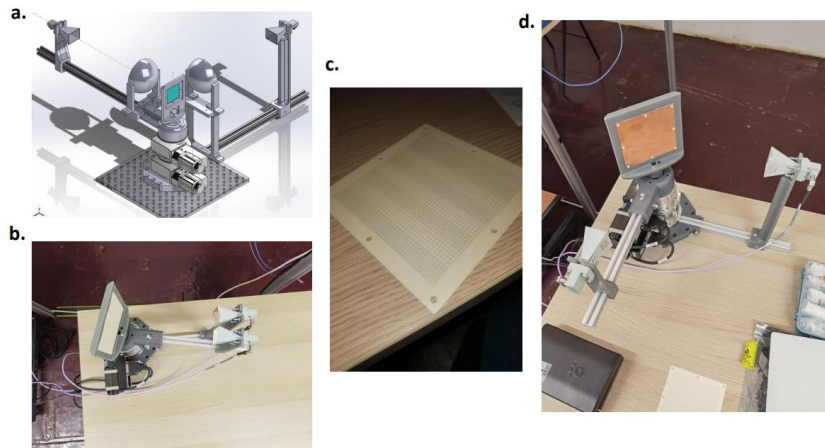
At present, GRW-1 is working on the design of a metasurface that operates in the sub 6 GHz frequency band and powered by a RFID frequency, which is shown below.



Wireless reconfigurable intelligent surface unit-cell prototype



GRW-1 is also collaborating with AAL-1, to develop a measurement testbed for reconfigurable intelligent surfaces (first figure below) based on non-Foster lumped elements.



a) A Schematic 3D view of the measurement setup, b) the remote-controlled rotating platform with our designed metasurface, and with d) the ground plane. c) The fabricated binary metasurface with four periods.

## 2.4 Contribution of WUP-1 – Overcoming Gap 1.4

The research project of WUP-1 is meant to address the research Gap 1.4 identified in the technical annex of the grant agreement. Specifically, since multiple-antenna systems are widely employed in wireless networks, but result in complex transceivers and high power consumption, metasurfaces can be used to provide similar performance, but at a lower power consumption. However, at present, low-complexity transmitter designs by metasurfaces are not available. In order to overcome Gap 1.4, a new generation of multi-stream transmitters that can operate with a single power amplifier must be developed. To this end, the considered approach is based on planar patterned metallic patches printed on F4B dielectric substrate and voltage-controlled varactor diodes to enable their reconfigurability at low cost and high switching rate. Specifically, two transmitter topologies that perform fast beam-hopping based on varactor diodes are being studied. Both are modulated metasurface antennas, where a transverse magnetic surface wave is launched and interacts with a periodically modulated boundary. This interaction is dictated by the tunable elements, which control the propagation constant of the radiating modes. In this way, the developed solutions are low-profile and flexible when it comes to determine the shape of the far-field beam. Moreover, they allow for the implementation of a simple control network, which is a key challenge when it comes to design reconfigurable metasurfaces.

In traditional designs, because of the presence of boundaries placed away from each other at distances of the order of the wavelength, transverse resonance forces the excited waves to be fast, thus achieving leaky-wave radiation. Instead, the innovative design developed by WUP-1 supports slow (or surface) waves. Therefore, they radiate only in the presence of a proper periodic modulation. In this way, the total field can be decomposed in modes defined in the transverse direction with respect to the propagation direction. For a certain frequency of operation, by designing a proper periodicity, these spatial harmonics are excited, and the transverse wavenumber shows that real power travels away from the antenna. Since there is leakage, the modes are complex solutions, with a real part describing a phase propagation along the surface, and an imaginary part which models the leakage (related to the transmitted beamwidth). The developed

methodology aims at showing how to flexibly control this complex propagation constant at the transmitter in a novel way, providing a wide field of view and a flexible control of the aperture field amplitude.

By studying a unit cell whose equivalent circuit is resonant in a periodic environment, is it possible to find a broad set of solutions of the resonance equation for the surface waves. In the case under consideration, the elements can be equivalently regarded as an LC circuit with small capacitances on top. Specifically, they consist of a metal cavity, which is filled by a dielectric, with a square slot etched on the upper wall and a central via. A tunable capacitance is connected across the slot and used to introduce a periodic modulation. In this way, it is possible to hit the resonance of the cells through voltage. In this region, a small capacitance growth strongly slows down the surface waves, and the range of operation of a commercial varactor is enough to define the impedance dynamic needed to significantly excite the -1 harmonic, which is the most significant one. As said before, since the lattice is small compared to the period, the previous solutions can be used to model the structure through a continuous variation of the impedance. By finding the proper structure, with such a simple methodology one can arrive to a low-profile design, with which the periodicity and the amplitude of this modulation can be reconfigured with a latency of tens or hundreds of nanoseconds, which is compatible with the latest communication systems.

The same methodology can be employed to design more complex modulated metasurface antennas. At the same time, a second topology, which consists of a double-layer metasurface is being studied. The design is composed of a variable impedance surface on top of a dielectric. The structure is backed with the previously described unit-cell. Thus, varactors are included as a load of the antenna. With this topology, beam-scanning is obtained by uniformly changing the impedance of the bottom circuit. Therefore, the top layer is responsible for the radiation, since it is the one that introduces the periodicity. Moreover, this design can achieve enough phase variation to steer the beam, because the diodes are tuned to work near the surface wave bandgap of the periodic structure. Meanwhile the periodicity remains unchanged, the guided wavelength is reconfigured, providing a much simpler solution that allows for a simplified biasing network.

Going back to the first topology developed by WUP-1, it must be highlighted that it presents no field of view limitation. Because of its scanning mechanism based on the reconfiguration of the period, the group velocity remains equal for all the configurations. This solution allows for flexible control of the radiation in terms of pointing angle, but also of beamwidth. Because of it, it is possible to tune how much the energy is confined towards the user, providing an advantage with respect to reconfigurable antennas based on PIN diodes. In contrast, a decline of the group velocity occurs in the second topology developed by WUP-1 (double layer metasurface). This implies a reduced operational bandwidth. Furthermore, this configuration also presents limited scanning range, due to the narrow set of achievable propagation constant values. Moreover, the far-field beamwidth cannot be controlled, because the reconfigurable elements are not included in the periodic layer. The last drawback has to do with the aperture illumination, since in the second topology we go closer or further apart from the resonance to scan, the attenuation constant of the leaky mode is different for every direction. Results show that this design cannot keep a stable aperture illumination for all the configurations. On the other hand, it brings a simple solution in terms of control complexity, which is one of the challenging issues when it comes to designing reconfigurable antennas. The most important advantage of the second design, despite all its drawbacks, has to do with the losses. Because the varactors do not define the modulation in the double layer design, the structure is less lossy. Moreover, working with two layers allows us to reduce and compress the range of operation of the varactors. This loss reduction, together with the implementation of a single control network, make the second developed topology a promising solution.

The results obtained by WUP-1 have resulted in the paper

J. García-Fernández, F. Caminita, C. Della Giovampaola, E. Martini, and S. Maci, *Reconfigurable Metasurface Antennas based on Varactor Diodes*, submitted for possible publication to the 2023 European conference of antennas and propagation (EuCAP).

### 3. Conclusions

The research activities concerning Task 1.1 are progressing as planned. All other ESRs have completed the initial literature review phase, which started in M7, and are currently developing innovative designs to tackle the specific challenge of their individual research project and close the corresponding research gap. In particular:

**AAL-1** has developed innovative metasurface solutions that provide a better angular stability than competing alternatives, while at the same time allowing to reflect both TE and TM incident polarizations, and operating over a broader frequency spectrum. These results have led to one publication, while a second publication is currently under preparation. In the second half of the project, the research activities of AAL-1 will focus on the refinement of the developed models, further improving the reconfiguration capabilities and performance of the developed metasurface structures.

**DEM-1** has developed innovative metasurface designs which operate above the sub 6GHz bands that is commonly used for wireless communications. The developed designs can support the use of carrier frequencies that are over twice as large as traditional carrier frequencies, and thus able to support information signals with a much larger bandwidth. In the second half of the project, the research activities of DEM-1 will focus on further increasing the carrier frequency that can be supported by the developed metasurface structures.

**GRW-1** has developed innovative metasurface architectures for operation in the millimeter wave frequency range, with reduced complexity and simplified control. The developed designs have validated by experimental measurements and resulted in two publications. The developed metasurface architecture is capable of supporting communication and sensing signals. In the second half of the project, the research activities of GRW-1 will focus more in detail on the analysis and implementation of the sensing task.

**WUP-1** has developed innovative designs for low-complexity metasurface structures that can be used to implement transmit modulation schemes thanks to limited complexity required to change their electromagnetic configuration in real-time. Reconfiguration latencies of tens or hundreds of nanoseconds have been achieved. These results have led to one publication. In the second half of the project, the research activities of WUP-1 will focus on further improving the reconfiguration capabilities and reducing the computational complexity of the developed metasurface designs.

### 4. Bibliography

- [1] C. Caloz and T. Itoh, *Electromagnetic Metamaterials: Transmission Line Theory and Microwave Applications*, John Wiley & Sons, Nov. 2005.
- [2] F. Capolino, *Theory and Phenomena of Metamaterials*, CRC press, Oct. 2009.
- [3] T. J. Cui, D. Smith, and R. Liu, *Metamaterials: Theory, Design, and Applications*, Springer, Nov. 2009.
- [4] A. Maier, *Handbook of Metamaterials and Plasmonics*, World Scientific, Dec. 2017.
- [5] S. B. Glybovski, S. A. Tretyakov, P. A. Belov, Y. S. Kivshar, and C. R. Simovski, *Metasurfaces: From microwaves to visible*, Physics Rep., vol. 634, pp. 1–72, May 2016.



- [6] H.-T. Chen, A. J. Taylor, and N. Yu, *A review of metasurfaces: physics and applications*, Rep. Prog. Physics, vol.79, no. 7, Jun. 2016.
- [7] A. V. Osipov and S. A. Tretyakov, *Modern Electromagnetic Scattering Theory with Applications*, John Wiley & Sons, Feb. 2017.
- [8] F. Liu, O. Tsilipakos, A. Ptilakis, A. C. Tasolamprou, M. S. Mirmoosa, N. V. Kantartzis, D.-H. Kwon, M. Kafesaki, C. M. Soukoulis, and S. A. Tretyakov, *Intelligent metasurfaces with continuously tunable local surface impedance for multiple reconfigurable functions*, Physics Rev. Applied, vol. 11, no. 4, Apr. 2019.
- [9] F. Liu, A. Ptilakis, M. S. Mirmoosa, O. Tsilipakos, X. Wang, A. C. Tasolamprou, S. Abadal, A. Cabellos-Aparicio, E. Alarcon, C. Liaskos, N. V. Kantartzis, M. Kafesaki, E. N. Economou, C. M. Soukoulis, and S. Tretyakov, *Programmable metasurfaces: State of the art and prospects*, IEEE Int. Symp. Circuits and Systems, May 2018.
- [10] S. V. Humand, J. Perruisseau-Carrier, *Reconfigurable reflectarrays and array lenses for dynamic antenna beam control: A review*, IEEE Transactions on Antennas and Propagation, vol. 62, no. 1, pp. 183–198, Jan. 2014.
- [11] J. B. Garcia, A. Sibille, and M. Kamoun, *Reconfigurable intelligent surfaces: Bridging the gap between scattering and reflection*, IEEE Journal on Selected Areas in Communications, vol. 38, no. 11, pp. 2538 – 2547, Nov. 2020.
- [12] S. W. Ellingson, *Path loss in reconfigurable intelligent surface-enabled channels*, 2021 IEEE 32nd Annual International Symposium on Personal, Indoor and Mobile Radio Communications (PIMRC), 2021
- [13] W. Khawaja, O. Ozdemir, Y. Yapici, F. Erden, M. Ezuma, and I. Guvenc, *Coverage enhancement for NLOS mmwave links using passive reflectors*, IEEE Open Journal of the Communication Society, vol. 1, pp. 263–281, Jan. 2020.
- [14] O. Ozdogan, E. Bjornson, and E. G. Larsson, *Intelligent reflecting surfaces: Physics, propagation, and pathloss modeling*, IEEE Wireless Communications Letters, vol. 9, no. 5, pp. 581 - 585, May 2020.
- [15] M. Di Renzo, F. H. Danufane, X. Xi, J. de Rosny, and S. A. Tretyakov, *Analytical modeling of the path-loss for reconfigurable intelligent surfaces - Anomalous mirror or scatterer ?*, 2020 IEEE 21st International Workshop on Signal Processing Advances in Wireless Communications (SPAWC), 2020.
- [16] Y. Cao and T. Lv, *Intelligent reflecting surface aided multi-user millimeter-wave communications for coverage enhancement*, 2020 IEEE 31st Annual International Symposium on Personal, Indoor and Mobile Radio Communications (PIMRC), 2020.
- [17] C. Chaccour, M. N. Soorki, W. Saad, M. Bennis, and P. Popovski, *Risk-based optimization of virtual reality over terahertz reconfigurable intelligent surfaces*, 2020 IEEE International Conference on Communications (ICC), 2020.
- [18] K. Ying, Z. Gao, S. Lyu, Y. Wu, H. Wang, and M.-S. Alouini, *GMD-based hybrid beamforming for large reconfigurable intelligent surface assisted millimeter-wave massive MIMO*, IEEE Access, vol. 8, pp. 19530 – 19539, 2020.
- [19] Y. Cao and T. Lv, *Delay-constrained joint power control, user detection and passive beamforming in intelligent reflecting surface assisted uplink mmwave system*, IEEE Transactions on Cognitive Communications and Networking, vol. 7, no. 2, pp. 482 – 495, June 2021

- [20] Y. Xiu, Y. Zhao, Y. Liu, J. Zhao, O. Yagan, and N. Wei, *IRS-assisted millimeter wave communications: Joint power allocation and beamforming design*, 2021 IEEE Wireless Communications and Networking Conference Workshops (WCNCW), 2021.
- [21] W. Chen, X. Ma, Z. Li, and N. Kuang, *Sum-rate maximization for intelligent reflecting surface based terahertz communication systems*, 2019 IEEE International Conference of Communications in China, 2019.
- [22] V. Jamali, A. Tulino, G. Fischer, R. Muller, and R. Schober, *Intelligent reflecting and transmitting surface aided millimeter wave massive MIMO*, Available: <https://arxiv.org/abs/1902.07670>, Feb. 2019.
- [23] M. Najafi and R. Schober, *Intelligent reflecting surfaces for free space optical communications*, IEEE Transactions on Communications, vol. 69, no. 9, pp. 6134 – 6151, Sep. 2021.
- [24] N. S. Perovic, M. Di Renzo, and M. F. Flanagan, *Channel capacity optimization using reconfigurable intelligent surfaces in indoor mmWave environments*, 2020 IEEE International Conference on Communications (ICC), 2020.
- [25] C. Pradhan, A. Li, L. Song, B. Vucetic, and Y. Li, *Hybrid precoding design for reconfigurable intelligent surface aided mmWave communication systems*, IEEE Wireless Communications Letters, vol. 9, no. 7, pp. 1041 – 1045, July 2020.
- [26] P. Wang, J. Fang, X. Yuan, Z. D. Chen, H. Duan, and H. Li, *Intelligent reflecting surface-assisted millimeter wave communications: Joint active and passive precoding design*, IEEE Transactions on Vehicular Technology, vol. 69, no. 12, pp. 14960 – 14973, Dec. 2020.
- [27] P. Wang, J. Fang, and H. Li, *Joint beamforming for intelligent reflecting surface-assisted millimeter wave communications*, Available: <https://arxiv.org/abs/1910.08541>, 2019.
- [28] H. Wang, Z. Zhang, B. Zhu, J. Dang, L. Wu, L. Wang, K. Zhang, and Y. Zhang, *Performance of wireless optical communication with reconfigurable intelligent surfaces and random obstacles*, Available: <https://arxiv.org/abs/2001.05715>, 2020.
- [29] W. Chen, et al. *Angle-dependent phase shifter model for reconfigurable intelligent surfaces: Does the angle-reciprocity hold?*, IEEE Communications Letters, vol. 24, no. 9, pp. 2060-2064, 2020.